

# Molecular Systems Design & Engineering

Accepted Manuscript



This article can be cited before page numbers have been issued, to do this please use: N. M. Cativa, M. S. Alvarez Cerimedo, J. Puig, G. F. Arenas, F. Trabadelo, M. A. A. Ayude, M. A. Zensich, G. M. Morales, W. F. Schroeder, H. E. Romeo and C. E. Hoppe, *Mol. Syst. Des. Eng.*, 2019, DOI: 10.1039/C8ME00085A.



This is an Accepted Manuscript, which has been through the Royal Society of Chemistry peer review process and has been accepted for publication.

Accepted Manuscripts are published online shortly after acceptance, before technical editing, formatting and proof reading. Using this free service, authors can make their results available to the community, in citable form, before we publish the edited article. We will replace this Accepted Manuscript with the edited and formatted Advance Article as soon as it is available.

You can find more information about Accepted Manuscripts in the [author guidelines](#).

Please note that technical editing may introduce minor changes to the text and/or graphics, which may alter content. The journal's standard [Terms & Conditions](#) and the ethical guidelines, outlined in our [author and reviewer resource centre](#), still apply. In no event shall the Royal Society of Chemistry be held responsible for any errors or omissions in this Accepted Manuscript or any consequences arising from the use of any information it contains.

**“Design, System, Application” statement**

This article proposes a new synthetic strategy for the generation of polymeric patterned films and coatings, characterized by the presence of oriented channels, through a process that combines two convenient strategies: cryogenic processing and visible-light photopolymerization. Combination of both techniques makes possible to obtain crosslinked polymeric films with the ability of conducting fluids (both hydrophobic and hydrophilic) in one direction (the freezing direction). Crosslinking the polymer by photopolymerization enables avoiding the use of expensive and time-consuming freeze-drying techniques for elimination of the ice used as template, which is an important advantage when compared with traditional cryogenic processing used, for example, for the synthesis of porous three-dimensional materials. Versatility of the proposed technique is demonstrated by showing its ability for obtaining systems with different channels sizes and morphologies. Moreover, the work also shows that nanostructures can confer photohermal properties to the final materials (among many other possible properties derived from nanostructure properties) increasing their potential applications to processes requiring heated environments. A wide variety of applications in the design of advanced platforms can be envisioned for these films based on their directionality. Among them we can mention advanced microfluidics, tissue growing, operations in micro-reactors, etc.

# Poly(ethylene glycol)-based cross-linked films with aligned micrometric channels: combining cryogenic processing and visible-light photopolymerization for the design of micro-patterned oriented platforms

Nancy M. Cativa,<sup>a</sup> M. Soledad Alvarez Cerimedo,<sup>a</sup> Julieta Puig,<sup>a</sup> Gustavo F. Arenas,<sup>b</sup> Fernando Trabadelo,<sup>c</sup> M. Alejandra Ayude,<sup>a</sup> Maximiliano A. Zensich,<sup>d</sup> Gustavo M. Morales,<sup>d</sup> Walter F. Schroeder,<sup>a</sup> Hernán E. Romeo,<sup>a,\*</sup> Cristina E. Hoppe<sup>a,\*</sup>

<sup>a</sup>*Nanostructured Polymer Division, Institute of Materials Science and Technology (INTEMA), University of Mar del Plata and National Research Council (CONICET), Av. J. B. Justo 4302, B7608FDQ Mar del Plata, Argentina*

<sup>b</sup>*LASER Laboratory - ICYTE - University of Mar del Plata and National Research Council (CONICET), Av. J. B. Justo 4302, B7608FDQ Mar del Plata, Argentina*

<sup>c</sup>*Electronics Laboratory, Institute of Materials Science and Technology (INTEMA), University of Mar del Plata (UNMdP) and National Research Council (CONICET)*

<sup>d</sup>*Chemistry Department, Universidad Nacional de Rio Cuarto-CONICET, Ruta Nac. 36 - Km. 601, X5804BYA, Río Cuarto, Córdoba, Argentina.*

\*Corresponding authors: [hromeo@fi.mdp.edu.ar](mailto:hromeo@fi.mdp.edu.ar); [hoppe@fi.mdp.edu.ar](mailto:hoppe@fi.mdp.edu.ar)

## ABSTRACT

Poly(ethylene glycol)-based cross-linked films with aligned micrometric channels were obtained by applying ice-templating processing and cryo-photopolymerization to aqueous solutions containing a methacrylate monomer and a visible light photo-initiator system. Aqueous solutions containing poly(ethylene glycol) dimethacrylate (PEG-dma), camphorquinone (CQ) and ethyl-4-dimethyl aminobenzoate (EDMAB) were casted between glass slides and unidirectionally frozen (horizontally) by imposing a temperature gradient along the ends of the sample holder, keeping one of the sample ends at sub-zero temperature and the other one at room temperature. Immediately after freezing, samples were cryo-photopolymerized and air-dried for obtaining patterned films with micrometric channels aligned in the freezing direction. Crosslinking enabled producing polymer films with high mechanical and chemical stability that did not dissolve or collapse by contact with solvents, allowing efficient flow of solutions along their oriented micro-structure. Due to the high anisotropy of the topography, flow was clearly unidirectional, as determined from microscopic observation of the liquid front movement after drop seeding, an effect absent in non-patterned films prepared from the same precursors but under isotropic freezing conditions. Aqueous solutions perfused the films forming a unidirectional front that advanced very fast along the freezing direction whereas hydrophobic solutions limited their flow to well-defined channels. Addition of nanostructures to the initial aqueous formulations allowed easy transferring of photothermal response to the aligned porous platforms. Through this strategy, remote localized heating of the films was attained by using a laser beam, which could be used to enhance the potentiality of these materials as chemical micro-reactors, responsive scaffolds and/or advanced microfluidic platforms.

## INTRODUCTION

Micro-patterning of a polymer surface is a very attractive and convenient way of changing the behavior of a film or coating for producing materials with sophisticated properties.<sup>1-7</sup> Inclusion of microscale topographies has been efficiently used in applications including cellular engineering,<sup>4,7</sup> microfluidics,<sup>1</sup> fog and water collection,<sup>8</sup> oil–water separation,<sup>9</sup> lubrication<sup>10,11</sup> and tuning of surface wettability<sup>12</sup> and antimicrobial activity of films.<sup>11,13</sup> Currently used techniques for micro-patterning include most types of lithographies and printing methods (photolithography,<sup>1</sup> electron and ion beam lithography,<sup>14</sup> soft lithography,<sup>15</sup> laser interference lithography,<sup>4,11</sup> dip-pen lithography, inkjet printing,<sup>16</sup> etc.) although unconventional techniques like those based on surface wrinkling<sup>17</sup> and controlled evaporation<sup>18</sup> are gradually gaining popularity because of the strong demand for simpler and less expensive procedures. As coffee ring stains have been the starting idea behind the development of evaporation-based micro-patterning techniques,<sup>19</sup> three-dimensional (3D) porous structures could be the inspiring muse for the development of patterning techniques based on the formation of regularly spaced grooves on coatings and films. This transition from porous polymers to patterned films would be a consequence of the reduction of dimension from 3D to 2D, transforming a pore into a groove. Hierarchical porous scaffolds envisioned for different applications (e.g., energy storage, tissue engineering, molecular filtration, controlled release, catalysis, bio-electrochemistry, among others) have been largely reported.<sup>20-23</sup> Porous materials have been pursued mainly because of their unique combination of extensive exposed surface area, low density and accessibility along the void volume. The demands for creating these advanced platforms have increasingly triggered the development of different structuring techniques, which range the processing of ceramic and polymer dispersions as well as polymer solutions.

Among these techniques, cost-effective ice-templating processes have been developed and explored as direct and versatile routes towards highly organized porous materials. In this context, directional freezing has become one of the most useful and powerful approaches.<sup>24,25</sup> The basic idea behind directional ice-templating relies on the segregation-induced arranging of a dispersed solid or solute by a solidifying solvent, driven by a strong temperature gradient imposed between the ends of the sample being frozen.<sup>26</sup> However, this deceptively simple process depends on the breakdown of the advancing solidification front, from planar to a non-planar (dendritic, columnar, lamellar) morphology. For this to happen, solid/liquid interface instability has to be induced, thus conditioning the final morphology and ice-crystal size that impacts consequently on the final size and morphology of the pore phase, which is a negative replica of the ice. While this structuring technique has mainly been used to create 3D porous architectures, only scarce literature can be found concerning 2D patterned films processed by directional freezing. Among the few studies that have attempted to translate the concept behind the directional freezing approach to a 2D scenario, only the use of colloidal NPs dispersions has been reported. In these examples, aqueous dispersions of NPs (TiO<sub>2</sub>, Au) were anisotropically frozen and then freeze-dried, rendering highly aligned 2D nanoparticle patterns on different substrates.<sup>27,28</sup> However, no studies concerning 2D polymeric films with aligned patterns have been reported on the field, which is really striking if we consider that several 3D polymer-based systems have been typically processed by directional freezing.<sup>29</sup> Hence, cryogenic procedures can be envisioned as a new tool for the generation of micro-patterns in 2D polymeric materials.

While it is true that a range of versatile techniques to obtain well defined patterns in polymer films are currently available, it is also true that special equipment facilities (not always cost-effective) are typically required. In the case of directional freezing approaches,

simple experimental setups are commonly needed, though energy-intensive and costly post-processing steps are typically required, involving freeze drying of the sample to remove the templating ice phase. These steps are required to avoid structure collapse during ice melting produced by dissolution of the polymer in the aqueous phase. The problem could be solved if the polymeric structure could be fixed by cross-linking and gelation previously to ice removal. Cross-linked polymers do not dissolve in contact with solvents and are usually characterized by better mechanical and structural properties, providing coatings with additional chemical and environmental resistance.<sup>30</sup> It is at this point that photopolymerization approaches appear as an interesting option to dispense with the usually long-term ice-removing steps involved in the ice-templating processes, which could make the 2D directional freezing strategy a potential candidate towards highly anisotropic films with tuned properties. Photoinitiated polymerization proceeds in the cryo-concentrated non-frozen liquid phase that surrounds the ice crystals, giving place to a crosslinked polymer around these crystals. When the system is defrosted, the ice crystals melt and a macroporous interconnected network with mechanical stability is obtained.<sup>31–33</sup> We recently showed that visible light cryo-photopolymerization can be applied to poly(ethyleneglycol)-dimethacrylate reactive solutions to obtain hydrophilic porous three-dimensional systems of high stability that do not dissolve in solvents.<sup>33</sup> These results support the idea of using this technique for obtaining crosslinked films avoiding freeze drying steps for ice removal.

Although applications of micro-patterned polymeric films are vast, versatility can be further enhanced by including nanostructures with the ability of presenting photothermal effect. It has already been demonstrated that dispersion of low amounts of metal NPs in a solid polymer can produce high temperature increases in the region of irradiation when

illuminated with light having a similar frequency than that corresponding to the resonance plasmon band (SPR) of the particles.<sup>34,35</sup> At SPR, light is converted very efficiently into heat by a process involving the increase in the population of “hot electrons” in the particle, transferring of this energy to the metal lattice (by coupling of the hot electrons with the lattice phonons) and subsequent decay to the environment.<sup>36–39</sup> Hence, in a low thermal conductivity medium (like in a solid polymer), the photothermal effect can produce high temperature increases at low irradiation powers and low NPs concentrations.<sup>34,35</sup> By modifying micro-patterned films with photothermal nanostructures, local heating can be induced by excitation with a laser or other light sources in a remote way. This ability is particularly interesting for the design of platforms with the potential of being used for more sophisticated or specific operations, like e. g. development of confined reactions in heated micro-environments, stimulation of cell growing at physiological conditions or development of microfluidic sensing/catalytic operations at specific temperatures, among many others.<sup>40,41</sup>

In this work, a simple and cost-efficient technique to produce patterned micro-channeled crosslinked polymeric films is proposed. The strategy is based on the combination of a cryogenic technique (directional freezing), commonly used for the development of unidirectional porosity and a photopolymerization procedure performed with visible light. Crosslinking under cryogenic conditions enables removal of water under atmospheric conditions and avoids the use of more expensive and time consuming freeze-drying steps. The influence of experimental conditions on the size and morphology of the grooves is analyzed, as well as the behavior of the channels regarding fluid transport. A final section describing addition of nanostructures to the initial formulations and activation of remote heating by taking advantage of the photothermal effect is also included.



## EXPERIMENTAL

### *Materials*

Silver nitrate ( $\text{AgNO}_3$ , P.A.), was acquired from Cicarelli and sodium borohydride ( $\text{NaBH}_4$ , 96 wt %) from Fluka. Poly(ethylene glycol)-dimethacrylate (PEG-dma,  $M_n=500$ ), camphorquinone (CQ) and ethyl-4-dimethyl aminobenzoate (EDMAB), sodium nitrate ( $\text{NaNO}_3$ ), potassium permanganate ( $\text{KMnO}_4$ ), sulfuric acid ( $\text{H}_2\text{SO}_4$ ), hydrogen peroxide  $\text{H}_2\text{O}_2$ , 11-mercaptoundecanoic acid (MUA, 95 wt %), gold(III) chloride trihydrate ( $\text{HAuCl}_4 \cdot 3\text{H}_2\text{O}$ , 99.5 wt %), tetrahydrofuran (THF) and poly(vinylpyrrolidone) (PVP,  $M_w=10000$ ), were purchased from Sigma-Aldrich. All reagents were used without further purification. For all the experiments carried out in this work, ultrapure water was used.

### *Preparation of patterned or non-patterned films*

Aqueous solutions of PEG-dma, CQ (2wt% respect to PEG-dma) and EDMAB (2wt% respect to PEG-dma) were prepared. In order to study the effect of water content on film surface features, three different water concentrations respect to PEG-dma were employed: 50, 80 and 90 wt%. Once prepared, solutions (100  $\mu\text{L}$ ) were drop casted and sandwiched between microscope glass slides to be then submitted to the freezing processing. Two different approaches were used. To obtain *non-patterned* films, isotropic freezing by sudden immersion of the slides in liquid nitrogen was accomplished. To prepare *patterned* films, microscope slides were subjected to horizontal directional freezing, imposing a longitudinal temperature gradient along the ends of the sample holder, keeping one of the sample ends at sub-zero temperature (in contact with a cold finger) and the other one at room temperature. Figure 1 depicts the setup used. For the patterned samples, and in order to evaluate the effect of the freezing driving force on surface features, two cooling sources were used: liquid nitrogen ( $-196^\circ\text{C}$ ) and a freezing mixture formed by

ice, salt (NaCl) and water (-15°C). After freezing was completed (5 min), samples (both patterned and non-patterned) were cryo-photopolymerized before ice melting, in order to preserve the induced surface morphology. For this, irradiation of the reactive mixture was carried out by means of an arrangement of blue LEDs (fixed 15 cm above the films - Figure 1) at a wavelength range of 410-530 nm and an irradiance of 600 mW/cm<sup>2</sup> (measured by using potassium ferrioxalate as actinometer). After structure crosslinking (2 min), samples were removed from the sample holders and then air dried at room temperature.

Films incorporating nanostructures were prepared by replacing the pure water in the initial formulation (80 wt%, respect to PEG-dma) by an equal amount of aqueous dispersions of nanostructures (see below). The procedure to obtain the patterned film was the same used for formulations without nanostructures.

### ***Synthesis of Nanostructures***

Ag@MUA nanoparticles (NPs) were synthesized as previously reported.<sup>42</sup> 20 mL of a solution of MUA in THF (100 mM) was added to 120 mL of a THF/H<sub>2</sub>O AgNO<sub>3</sub> solution (8.33 mM) under vigorous stirring. After 5 min, 10 mL of a freshly prepared NaBH<sub>4</sub> aqueous solution (1M) was rapidly added. The black solid formed was separated by decantation, dispersed in 20 mL of distilled water and annealed by refluxing at T ≈ 140 °C for 24 h. After this process was finished, NPs dispersion was centrifuged and purified through precipitation/ dispersion cycles. The final product was dispersed in 20 mL of distilled water until obtaining a dispersion with a Ag concentration of ≈ 5 mg /ml.

An aqueous dispersion of graphene oxide (GO) was prepared from oxidation of graphite flakes using a modification of Hummers and Offeman's method.<sup>43</sup> In a typical reaction, 0.5 g of graphite flakes, 0.5 g of NaNO<sub>3</sub>, and 23 mL of H<sub>2</sub>SO<sub>4</sub> were stirred

together in an ice bath. Next, 3 g of  $\text{KMnO}_4$  was slowly added maintaining the temperature below 5 °C. After complete dispersion, the mixture was transferred to a water bath and maintained at 5 °C under stirring for about 12 h until forming a thick paste. Afterwards, the paste was added to 400 mL of iced-water, and the mixture was stirred for 30 min, keeping all the time the temperature below 5 °C. Finally, 100 mL of a cold ( $\approx 0$  °C) aqueous solution of  $\text{H}_2\text{O}_2$  (3%) was added. The resulting mixture was allowed to decant, then the supernatant was discarded and the remaining precipitated material re-dispersed in water (400 mL). The decantation process was carried out into a refrigerator ( $\approx 5$  °C) and repeated until the precipitation process becomes difficult. Then, the purification was continued by centrifugation (4000 rpm for 30 min) until the pH of the supernatant was approximately 4. Finally, the resulting dispersion was dialyzed (dialysis membrane of regenerated cellulose with a molecular weight cut-off around 12–14 kD; Spectra/Por®) against water (18 M $\Omega$  cm) until no changes in conductance of the solution were observed for 6 h after dialysis process. The purified dispersion was concentrated by centrifugation until obtaining a dispersion with a concentration of  $\approx 3$  mg/mL. The final sample was stored in absence of light at 2–5 °C in the refrigerator for at least 60 days before its use.

Gold branched plates were prepared in a one-step process at mild temperatures as previously reported.<sup>44</sup> Briefly, a certain volume of an aqueous solution of  $\text{HAuCl}_4$  (0.02 M) was added to 10 mL of a diluted aqueous solution of PVP (0.004 M). After homogenization, the mixture was heated up to 70 °C and left standing without stirring for 16 h. Then, the final reaction mixture was cooled to room temperature and several cycles of decantation and centrifugation carried out to increase its final concentration up to 1 mg/ml of Au.

### ***Characterization Techniques***

Overall film conversions were determined by Fourier-transformed infrared spectroscopy (FTIR) in the near infrared region, from the intensity of the methacrylate band at  $6165\text{ cm}^{-1}$ .

Transmission optical microscopy (TOM) micrographs were taken using a Leica DMLB microscope provided with a video camera (Leica DC 100). Video clips of the imbibition process were also recorded.

A concentrated aqueous solution of crystal violet (CV) dye and a hydrophobic blue permanent ink were used to imbibe the micrometric channels of the patterned films prepared with 80 wt% of water respect to PEG-dma. A droplet of the dye solution and a droplet of the tip of the marker were placed onto the film surface for seeding.

A 1W DPSS laser centered at 532 nm (SDL-532-1000T Shanghai Dream Lasers Technology Co. Ltd.) was used to study the photothermal response of patterned films prepared with 80 wt% of the nanostructures dispersions respect to PEG-dma. Temperature was recorded using a Fluke Ti32 Infrared Camera with IR-Fusion<sup>®</sup> technology. The laser power at the irradiation spot was about  $75\text{-}80\text{ mW/cm}^2$ .

Transmission electron microscopy (TEM) images of Ag@MUA NPs and gold branched plates were obtained with a Philips CM-12 microscope operated at 100 kV. Samples were prepared by evaporating a drop of the dispersion on a copper grid coated with Formvar and a carbon film.

Scanning electron microscopy (SEM, JEOL JSM-6460LV) was used to obtain micrographs of GO. Samples were previously coated with a fine layer of Au–Pd.

## RESULTS AND DISCUSSION

### *Design of the experimental setup*

The strategy proposed in this work combines directional freezing (a cryogenic technique) and cryo-photopolymerization for obtaining crosslinked films with anisotropic features (oriented grooves). As mentioned before, the directional freezing technique has been mainly applied for obtaining 3D monoliths by slow vertical immersion of dispersions (or solutions) in a cryogenic liquid, most often using cylindrical molds as containers. However, to obtain a film, a different setup must be designed that enables a horizontal temperature gradient to be imposed on a surface along only one direction. (Figure 1)

In this case, the temperature gradient was longitudinally imposed along the ends of the sample holder by using a flat metallic cold finger (an aluminum bar) cooled with a cryogenic liquid (liquid nitrogen). The cold finger maintained one of the ends of the film substrate at sub-zero temperature (in this case, at  $-35^{\circ}\text{C}$ ) whereas the other one was kept at room temperature ( $17^{\circ}\text{C}$ ). The difference in temperature between both ends provoked the advance of the ice front from the coldest end to the extreme maintained at room temperature. Parameters like e.g. the temperature of the cryogenic liquid, the thermal conductivity of the cold finger, the area and thickness of the liquid sample, etc. can be adjusted to control the temperature gradient imposed on the aqueous solution/dispersion. Total void fraction and developed morphologies (channel size and geometry) are expected to depend accordingly on the initial formulation (concentration of the reactive acrylic blend in the aqueous dispersion), the viscosity of the solution, the temperature gradient and the freezing rate imposed.

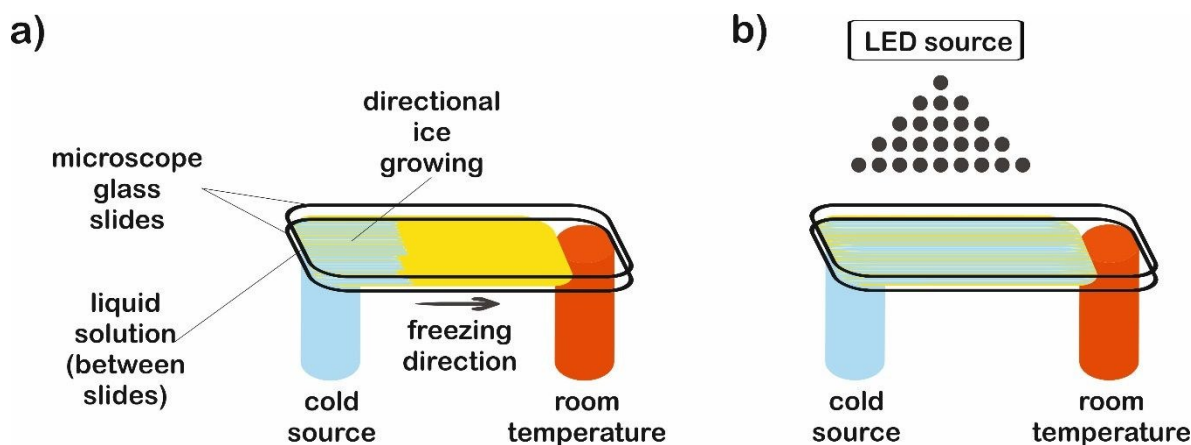


Figure 1. Schematic representation of the setup used for the development of a temperature gradient on films formed from aqueous solutions of the reactive, photopolymerizable system. (a) Temperature gradient imposed on liquid films induces unidirectional freezing and development of oriented columns of ice. (b) Photopolymerization is initiated by irradiating the semi-frozen system with a blue LED source.

### *Synthesis of the platforms*

Patterned films were obtained by freezing a fixed volume of an aqueous dispersion of the reactive blend (PEG-dma + CQ + EDMAB) between two microscope slides. For easy detachment after crosslinking, the top glass slide was covered with <sup>®</sup>Parafilm. Samples were submitted to a temperature gradient using the setup depicted in Figure 1a, keeping the cold end at  $-35^{\circ}\text{C}$ . After only a few seconds, a clear development of an ice front was observed. This front advanced towards the hottest end and stopped when the temperature reached  $0^{\circ}\text{C}$ . Hence, the length of the film was defined by the region of temperatures comprised between  $-35^{\circ}\text{C}$  and  $0^{\circ}\text{C}$  that, in this case, was about 2 cm. After 5 minutes, the film was in a semi-frozen<sup>31,32</sup> state. In order to preserve the developed morphology, radical photopolymerization was immediately carried out by attaching an arrangement of blue LEDs to the freezing setup (Figure 1b). The films were irradiated with blue light by placing

the source 15 cm above the film. The initiating mechanism has been discussed in the literature and is briefly described here.<sup>45</sup> Visible-light irradiation produces the excitation of CQ to its singlet, which rapidly undergoes intersystem crossing to the triplet state. The excited triplet is reduced by EDMAB to give rise to ketyl and  $\alpha$ -amino free radicals. The amino radical initiates the radical polymerization of PEG-dma while the ketyl radical is not an efficient initiator and dimerizes.

The progress of the photopolymerization was monitored by following the decrease in absorbance of the characteristic near-IR band of methacrylate groups centered at 6165  $\text{cm}^{-1}$ , assigned to the  $=\text{CH}_2$  first overtone (Figure S1).<sup>46</sup> The polymerization kinetics of PEG-dma was strongly influenced by the reaction temperature. While full conversion of methacrylate groups was achieved after 2 minutes of irradiation at room temperature, only a conversion of 0.38 was achieved after the same time of irradiation at  $-35\text{ }^\circ\text{C}$ . This behavior is attributed to the fact that free-radical polymerization becomes diffusion limited at subzero temperatures, due to two main effects: a decrease in the initiator efficiency and the trapping of propagating radicals in the network.<sup>47</sup> In addition, the presence of crystallized monomer (PEG-dma) at  $-35\text{ }^\circ\text{C}$  reduces the ultimate degree of conversion. However, when the sample irradiated at  $-35\text{ }^\circ\text{C}$  for 2 min was defrosted and stored for several hours at room temperature, polymerization continued in the dark until almost full conversion of methacrylate groups (Figure S1), due to the recovery of mobility of trapped radicals in the network. In this way, complete conversion was attained by simply storing the sample during a few hours at room temperature.

When used with common thermoplastic polymers or ceramic/nanostructured colloids, the directional freezing processing usually involves a final step of freeze drying. This step is required for removing ice without risk of structure collapse. In our case, as

photopolymerization crosslinks the structure, this time-consuming, expensive step was not necessary. By simple air drying at room temperature, ice was melted and evaporated, giving place to the formation of a crosslinked, grooved polymeric structure with good mechanical and solvent stability. Before analyzing the properties and potential use of these films, it is important to elucidate the developed morphology during the processing and its dependence on some of the experimental parameters. In the following section, results from structural characterization of the films are analyzed.

### *Structural characterization*

Transmission optical microscopy (TOM) characterization was carried out on obtained films after drying, for samples containing different amounts of water in the initial formulation. When a cryogenic technique is used to obtain a macroporous material, water content is a key parameter that mainly controls the final degree of porosity, although some effects on pore size can also be observed as a function of the solution viscosity. In our case, the size of the channels increased with the water content, indicating that thicker ice columns were formed when 2D freezing was performed on more diluted solutions. Figure 2 shows TOM micrographs of films obtained with 50, 80 and 90 wt% of water in the initial reactive aqueous solution. Brighter regions in the micrograph were associated with the presence of grooves (regions with a lower amount of solid material are characterized by a higher transmittance than the rest of the film). As clearly shown, all formulations enabled to obtain films characterized by the presence of well-developed patterns oriented in the freezing direction. As mentioned, the diameter of these channels markedly differs from one formulation to another. For 50 wt% of water, an average channel size of  $6.6 \pm 1.5 \mu\text{m}$  was obtained, whereas for 80 and 90 wt% of water, the average sizes were  $12.4 \pm 2.7 \mu\text{m}$  and



$18.3 \pm 4.0 \mu\text{m}$  respectively (Figure S2). These results markedly differed from that found for a sample obtained under conditions of isotropic (non-directional) freezing. This isotropic freezing was attained by direct and sudden contact of the whole sample (containing 80wt% of water) with liquid nitrogen. Figure 3 shows a TOM micrograph of this sample in which a disordered structure of voids can be observed. This structural change indicates that imposition of a thermal gradient is required for directional freezing and micro-patterning of the films.

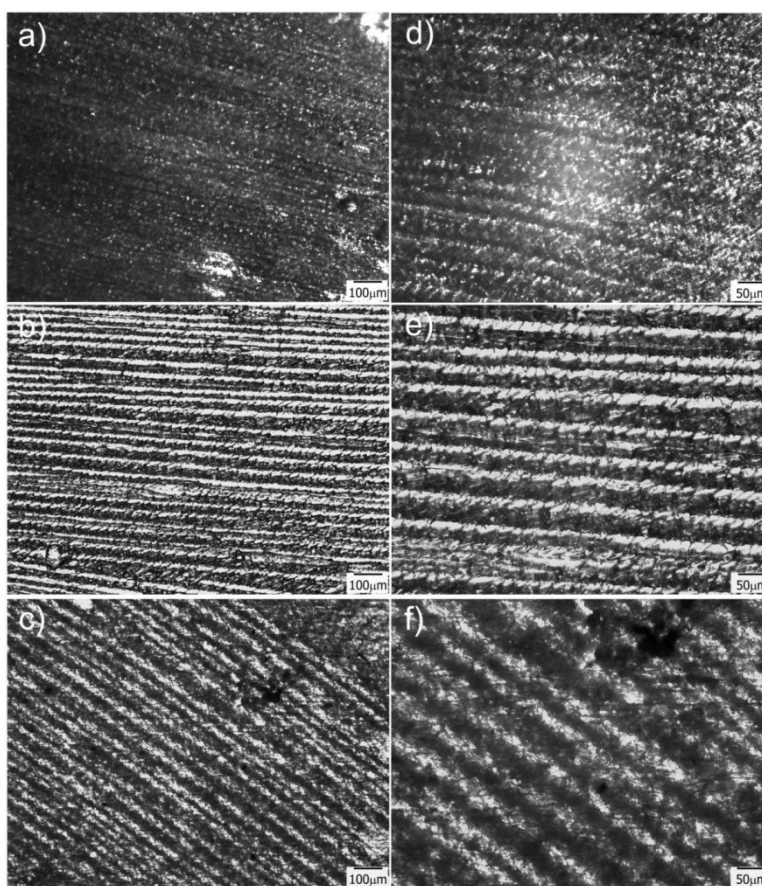


Figure 2. TOM micrographs of films obtained for 50 (a,d), 80 (b, e) and 90 (c, f) wt% of water in the initial formulation; d, e and f are magnifications of a, b and c respectively taken from the central part of the image. Brighter regions correspond to the grooves.

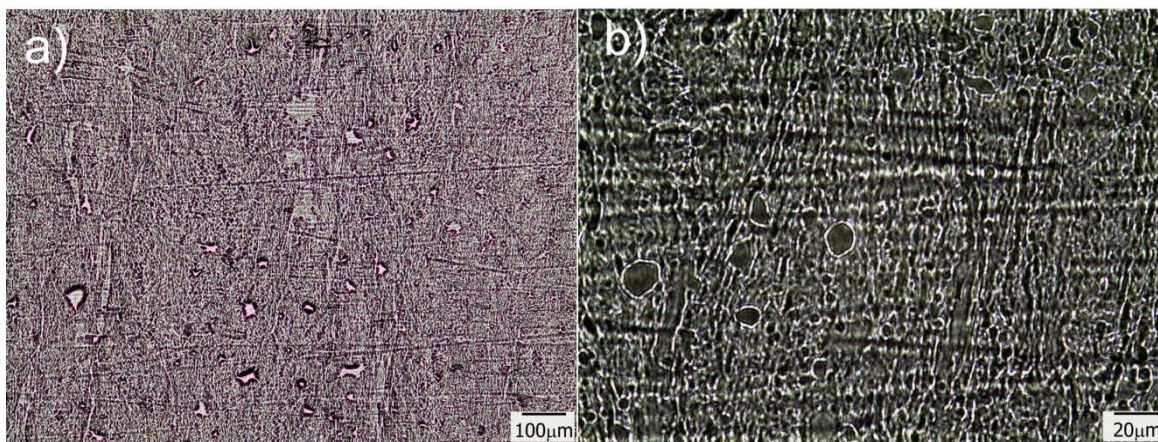


Figure 3. TOM micrographs obtained for a sample containing 80wt% of water and submitted to isotropic freezing; b is a magnification of a taken from the central part of the image.

Another important parameter in structuring cryogenic techniques is the freezing rate. In order to evaluate the effect of a lower freezing rate on the obtained morphologies, the cryogenic liquid was changed from liquid nitrogen ( $-196^{\circ}\text{C}$ ) to a freezing mixture formed by ice, salt and water ( $-15^{\circ}\text{C}$ ). By imposing a lower temperature gradient on the sample, a modification in the morphology of the structure was expected. In effect, an increase in the size of the oriented patterns was obtained according to the new solidification driving force (Figure 4). In this case, the average size was  $66 \pm 14 \mu\text{m}$ , a much higher value than those obtained using liquid nitrogen (Figure S2). However, this increase in size was accompanied by a change in morphology. As was revealed, each one of the longitudinal patterns exhibited features (localized instabilities) perpendicularly oriented with respect to the main freezing direction (magnification of Figure 4a). The formation of these secondary instabilities can be explained on the basis of the ice segregation phenomenon itself. When the ice is formed during the primary segregation event (along the main freezing direction), lateral expulsion of the (in our case) PEG-dma/photo-initiator mixture (still containing

water) occurs. This leads to the concentration of monomers and photo-initiators between primary ice crystals, and, depending on the freezing rate, a secondary lateral expulsion may occur. If the freezing rate is low enough, time is provided to the expelled phase (PEG-dma + photoinitiators + water) to undergo a secondary segregation event, this time up and down respect to the forming ice. Under this circumstance, patterns oriented perpendicularly to the main freezing direction are generated, as clearly seen in Figure 4. This effect was absent when the employed freezing rate was higher (that is, by using liquid nitrogen as the cooling source). These secondary formations would induce flow tortuosity effects along the patterns, leading to a more difficult accessibility of the channels. Although at first sight this change can be considered as a disadvantage, this morphology could be potentially useful for separation or chromatographic operations requiring higher tortuosity. Hence, modification of the freezing conditions can be an interesting tool to enhance the versatility of the obtained films in applications that require patterns at different scales. Experiments designed to elucidate conditions conducting to special changes on the morphology of the channels are currently under way.

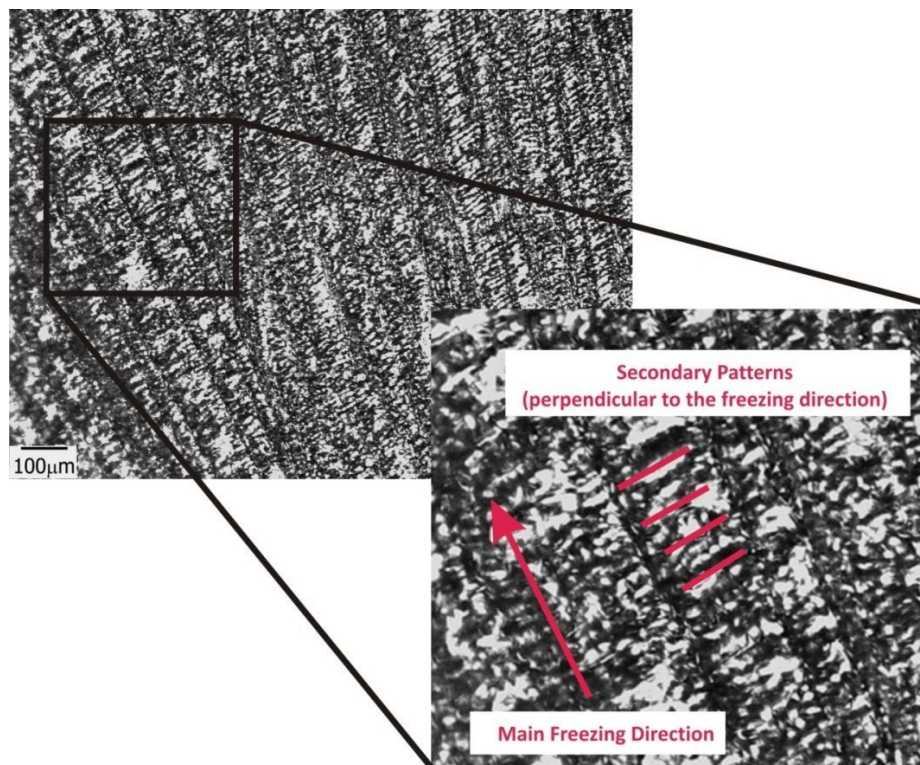


Figure 4. TOM micrographs of films obtained for 50 wt% of water in the initial formulation frozen using a freezing mixture formed by ice, water and salt.

#### *Unidirectional flow*

The as prepared patterned films were used as guiding platforms to induce directional liquid flow. The presence of anisotropic surface structures could restrict liquid flow to a desired direction, which has potential interest in microfluidics,<sup>1</sup> fog harvesting,<sup>8</sup> lubrication,<sup>10</sup> etc. Surface chemistry (hydrophilicity degree of the surface channel) is also a variable controlling the flow and pinning of the liquid, as well as the geometry and aspect ratio of the channel itself.<sup>48</sup> In this case, a polar (crystal violet dye) and a non-polar (permanent marker ink) solutions were employed in imbibition experiments to reveal both differences in wettability and unidirectional (or not) behavior of the running solution. Complete and instantaneous liquid spreading occurred for all sample surfaces. This is an

expected result, as inclusion of a high porosity volume decreases the apparent contact angle of the surface.<sup>49</sup> The results also demonstrated that both solutions were successfully imbibed and flowed unidirectionally on the patterned films. However, some differences could still be found between the behaviors of both kinds of liquids. In the case of hydrophobic permanent marker ink (Figure 5), it can be clearly seen how, by constraining the drop seeding point, the liquid can be induced to flow along the oriented pattern, avoiding at the same time that the moving phase steps out of the channel, which results extremely interesting for applications in which precise micrometric control of liquid “tributaries” is needed. This property can also be used for precisely patterning hydrophobic barriers in the hydrophilic platform, which can be useful for imposing delimitation to the channeled system, outside which the liquid will not be able to flow. Permanent markers have already been successfully used for the creation of such barriers in paper microfluidics devices.<sup>50,51</sup>

For polar liquids, like the CV dye aqueous solution used in this experiment, the behavior was different. Due to that the substrate is hydrophilic, restraining seeding to one point and flowing to only one channel was not possible. This is because of the unavoidable degree of swelling and lateral diffusion that occur after dropping of the liquid on the patterned system. When the aqueous solution was dropped on a substrate point, immediately perfused all the film, provoking a strong and fast unidirectional advance of the aqueous front along the freezing direction (Figure 5 and movie-1 in SI). This perfusion and fast advance of the liquid front is quite similar to which occurs in the case of paper and other hydrophilic porous substrates but with the interesting advantage of occurring along a particular direction (the freezing direction). Due to the versatility of the proposed strategy, that enables the use of a variety of acrylic monomers, hydrophilicity of the matrix (and its

flow behavior) could be controlled by changing the formulation of the initial reactive mixture, which enhances the potential interest of these films for diverse applications. Moreover, fabrication of hydrophobic barriers to limit flow to a selected region of the substrate could be carried out, in a similar way to which is performed in paper microfluidics devices.<sup>52</sup>

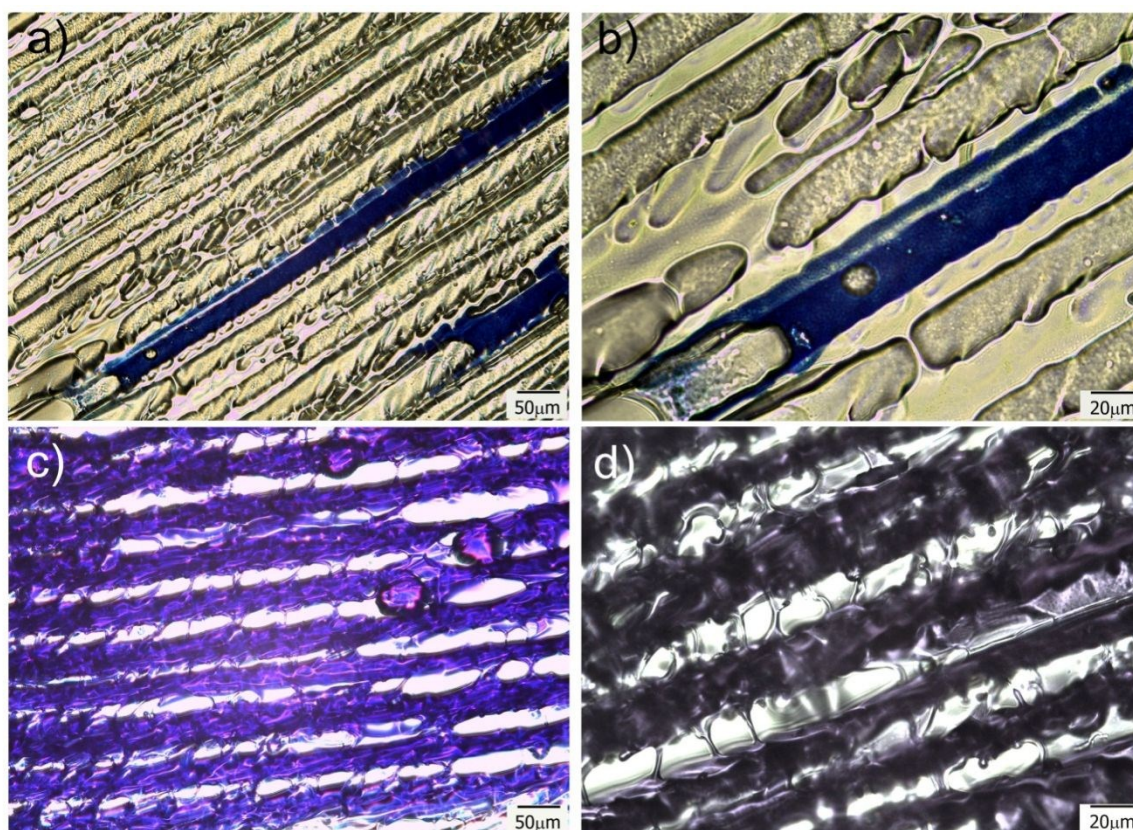


Figure 5. (a-b) TOM images of a marker ink drop running along a channel. (c-d) TOM images of a CV aqueous solution running along parallel channels. Both sets of experiments were done with the film prepared from 80 wt% water.

Taking advantage of these properties, and envisioning a potential use of the prepared platforms as guiding substrates to finely dose, for instance, chemical reactants, a proof-of-concept test was carried out to evaluate the possibility of inducing a chemical

reaction between  $\text{NaBH}_4$  and  $\text{HAuCl}_4$  in the film, with the consequent production of gold nanoparticles at the reactants meeting region. Figure 6 shows the results of this simple experiment consisting in first dispensing a drop of  $\text{HAuCl}_4$  aqueous solution on the right handed end of the film and, immediately after, a drop of  $\text{NaBH}_4$  on the left handed end. Both liquids fronts advanced to the center of the film and NPs were formed in the region in which they overlapped, as inferred from the appearance of the red-dark color better observed by TOM (Figure 6). As the seeding lines were not carefully defined (solutions were simply dropped with a pipette on the film surface), the overlapping region was not straight but sawed.

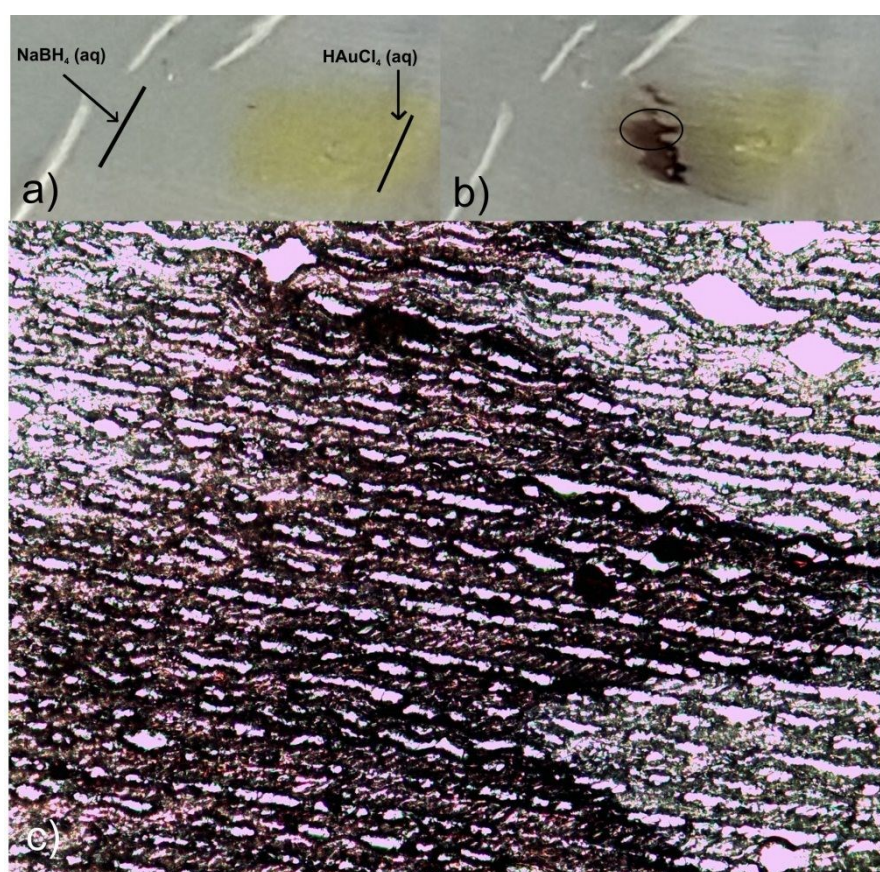


Figure 6. Digital pictures showing the meeting of two reactants ( $\text{HAuCl}_4$  and  $\text{NaBH}_4$  aqueous solutions) seeded on opposite sides of the film. The obtained product was Au NPs

(dark red zone). The initial step involved dropping of the  $\text{HAuCl}_4$  solution on the right end of the film (a), followed by dropping of  $\text{NaBH}_4$  and encounter of both reactants to give Au NPs (b). Formation of NPs can be observed as a red-dark sawed region by TOM (c).

### *Photothermal Heating*

To provide the films with the ability of being remotely heated, different aqueous dispersions containing photothermal nanostructures (GO, gold branched structures and Ag NPs) were added to the initial reactive solution (TEM/SEM images of these structures are available in Figure S3). Specific nanostructures presenting extended plasmon bands in the whole vis-NIR spectrum were specifically selected with the idea of conferring the films with light sensitivity in a wide range of wavelengths. GO and gold branched plates present wide absorptions that start at about 500 nm and extend until the NIR range (Figure S4a-b). On the other hand, plasmon band of Ag@MUA NPs present pH sensitivity due to the presence of carboxylate groups on their surface (Figure S4c). Partial protonation of these groups enables the formation of aggregates of controlled sizes that absorb in different regions of the spectrum.

To prepare the films, water in the reactive mixtures (80wt%) was replaced by colloidal dispersions of the nanostructures and then frozen and photopolymerized in the usual way. Figure 7 shows TOM micrographs of samples obtained with similar amounts of GO, gold branched structures and Ag NPs. As clearly observed, size of the pores did not change with the addition of any of the nanostructures to the initial formulation. However, all samples show the presence of micrometric objects dispersed in the micro-patterned film that can be attributed to some degree of nanostructures aggregation. This aggregation is probably a consequence of the cryogenic processing: when ice is formed, colloidal



nanostructures are expelled to a highly concentrated water phase containing the monomer and the initiator system. This change in concentration and dielectric constant of the medium can affect the stability of the particles and induce the formation of aggregates. This moderate aggregation extent (not macro segregation was observed in any of the cases) did not preclude channel formation or photothermal activity of the films. Table 1 shows the thermal response of samples after irradiation with a green laser (centered at 532 nm) during 90 sec. This irradiation wavelength was selected with the idea of using an optical excitation not specifically favorable for any of the structures. In fact, this irradiation wavelength is in a low absorbance range for the three kinds of nanostructures and can be considered as one of the less favorable conditions for activation (see Figure S4) However, as can be observed in Table 1, all samples show a significant localized temperature increase in the irradiation zone. The highest value was found for films modified with GO and the lowest one for films obtained using Ag NPs. A priori, these differences are not easy to correlate with the type of structure used to modify the film, for several reasons. First of all, absorption of the initial dispersions differed between structures as can be inferred from differences between spectral behaviors (Figure S4). Moreover, these spectra are modified (typically red-shifted and damped) by aggregation, as a consequence of dipolar interaction present between structures. Finally, local variation in the concentration of the samples within the film can also alter the intensity of the absorption producing a modification of the capacity of the system for being heated. All these variables show that a precise prediction of the response of the films obtained with different nanostructures can be a very complex issue that would deserve further work. At this point which is important to remark is that, even under non-ideal irradiation conditions, an important photothermal effect was observed in all cases. This result highlights the efficient conversion from light to heat that can be attained by

inclusion of plasmonic nanostructures in solid matrices with low thermal conductivity (like crosslinked polymers) and also opens the way to the possibility of remotely activate temperature-dependent local processes in patterned channels.

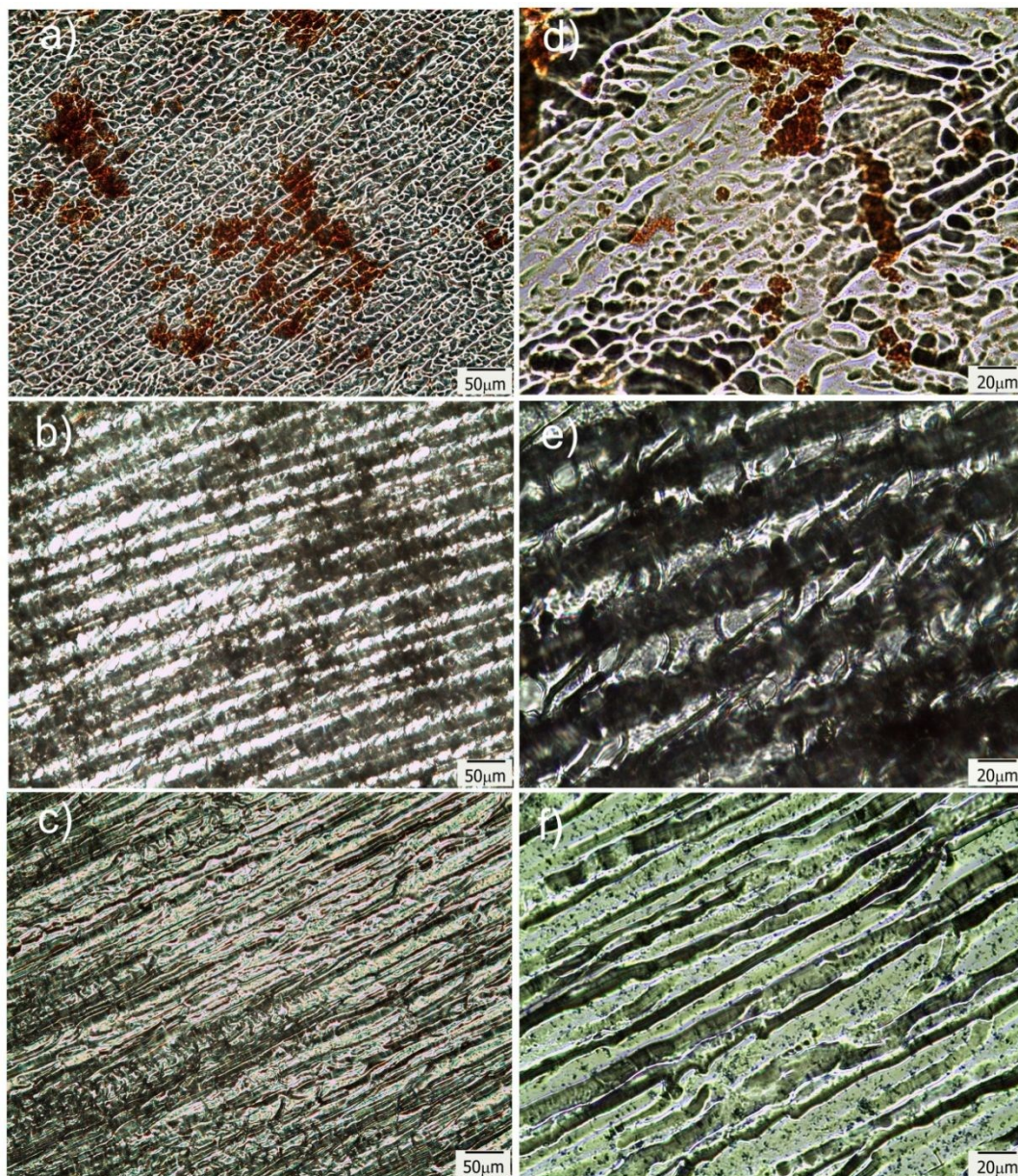


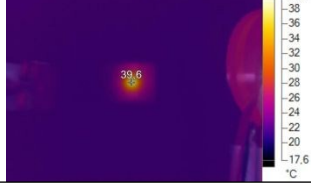



Figure 7. TOM micrographs of films modified with Ag@MUA NPs (a,d), GO (b, e) and Au branched plates (c, f); d, e and f are magnifications of a, b and c respectively.

**Table 1.** Maximum temperature attained after 30, 60 and 90 seconds of irradiation of the films with a green laser. The last column also shows the thermographic images corresponding to 90 sec of irradiation.

| Sample                           | Irradiation Time (sec) |            |  |
|----------------------------------|------------------------|------------|--|
|                                  | 30s                    | 60s        | 90s  |
| <b>Neat</b>                      | 22.0<br>°C             | 22.0<br>°C | <b>22.1 °C</b><br>   |
| <b>With Ag@MUA NPs</b>           | 25.2<br>°C             | 26.0<br>°C | <b>26.7 °C</b><br>  |
| <b>With GO</b>                   | 36.6<br>°C             | 36.3<br>°C | <b>39.6 °C</b><br> |
| <b>With Gold Branched Plates</b> | 27.7<br>°C             | 29.5<br>°C | <b>30.2 °C</b><br> |

## CONCLUSIONS

Micro-patterned oriented platforms, based on the cryogenic processing and photopolymerization of poly(ethylene glycol)-dma solutions, were successfully obtained by a convenient and cost-efficient technique. Structure and size of the channels were

controlled by changing the freezing conditions and the amount of water in the initial solutions, which enabled obtaining patterns with different topographies. Unidirectional flow showed to be possible for both aqueous and non-polar solvents, an effect absent in non-patterned films. Aqueous solutions perfused the films forming a unidirectional front that advanced very fast along the freezing direction. On the contrary, hydrophobic solutions limited their flow to well-defined channels indicating that channel walls acted as efficient barriers for liquid transport. Inclusion of nanostructures in the initial aqueous formulations added photothermal responsiveness to the micro-patterned films. Remote localized heating was attained by using a green laser, which could be used to enhance the potentiality of these materials as chemical micro-reactors, responsive scaffolds and/or advanced microfluidic platforms.

### Acknowledgements

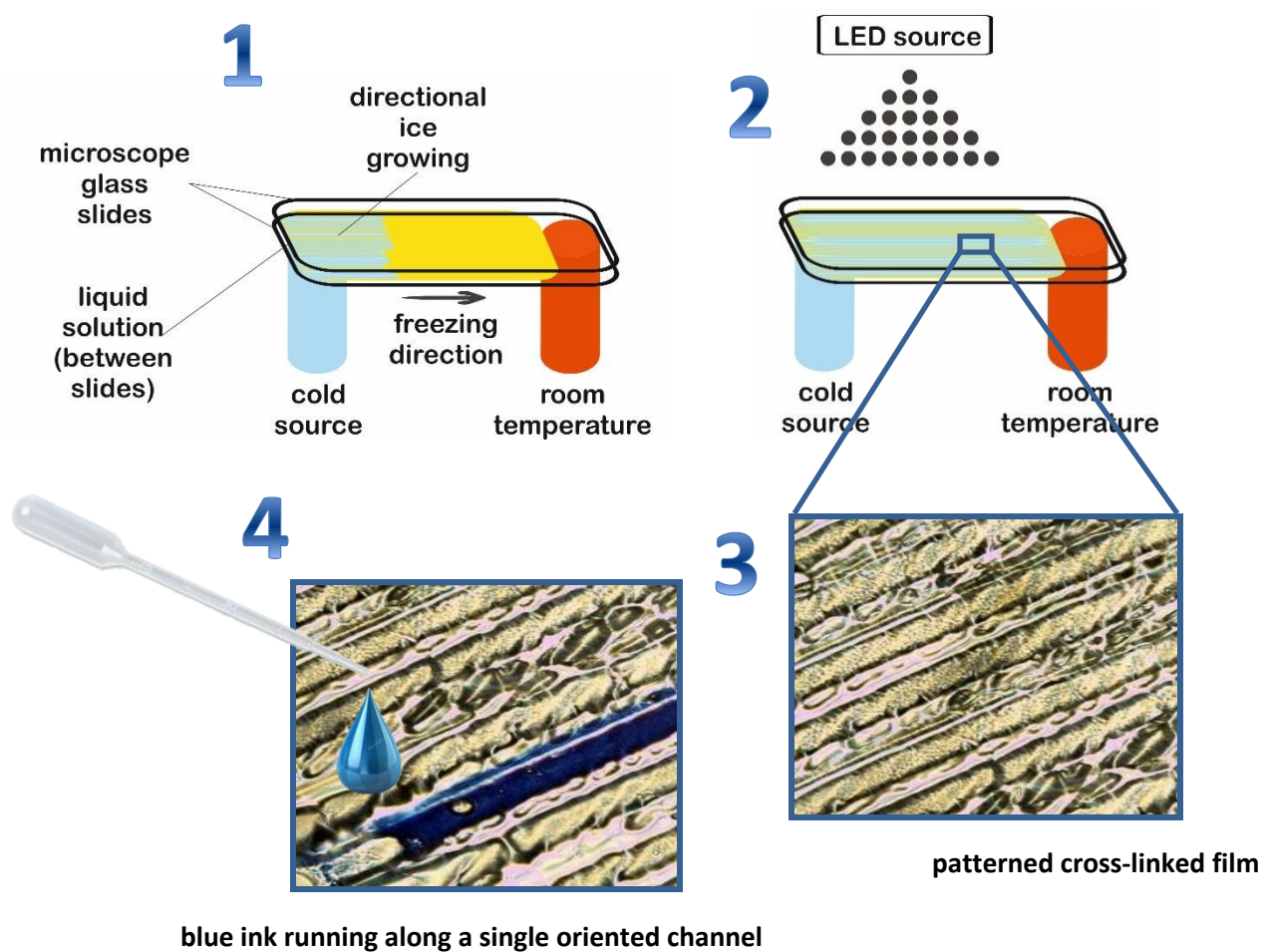
Financial support by ANPCyT (PICT 2015-1433), CONICET (PIP N° 0594) and UNMdP is gratefully acknowledged.

### REFERENCES

- 1 S. Gao, W.-T. Tung, D. S.-H. Wong, L. Bian and A. P. Zhang, *Journal of Micromechanics and Microengineering*, 2018, **28**, 095011.
- 2 O. Brazil, V. Usov, J. B. Pethica and G. L. W. Cross, *Microelectronic Engineering*, 2017, **182**, 35–41.
- 3 L. Xu, A. E. Seline, B. Leigh, M. Ramirez, C. A. Guymon and M. R. Hansen, *Otology & Neurotology*, 2018, **39**, 119–126.
- 4 D. Barata, P. Dias, P. Wieringa, C. van Blitterswijk and P. Habibovic, *Biofabrication*, 2017, **9**, 035004.
- 5 Y. Zhao, R. Truckenmuller, M. Levers, W.-S. Hua, J. de Boer and B. Papenburg, *Materials Science and Engineering: C*, 2017, **71**, 558–564.
- 6 M. P. Prabhakaran, E. Vatankhah, D. Kai and S. Ramakrishna, *International Journal of Polymeric Materials and Polymeric Biomaterials*, 2015, **64**, 338–353.
- 7 A. D. Sharma, S. Zbarska, E. M. Petersen, M. E. Marti, S. K. Mallapragada and D. S. Sakaguchi, *Journal of Bioscience and Bioengineering*, 2016, **121**, 325–335.
- 8 M. Gürsoy, M. T. Harris, A. Carletto, A. E. Yaprak, M. Karaman and J. P. S. Badyal, *Colloids and Surfaces A: Physicochemical and Engineering Aspects*, 2017, **529**, 959–965.

- 9 C. Chen, P. Xu and X. Li, in *2015 Transducers - 2015 18th International Conference on Solid-State Sensors, Actuators and Microsystems (TRANSDUCERS)*, IEEE, Anchorage, AK, USA, 2015, pp. 347–350.
- 10 K. Hiratsuka, A. Bohno and H. Endo, *Journal of Physics: Conference Series*, 2007, **89**, 012012.
- 11 A. Rosenkranz, M. Hans, C. Gachot, A. Thome, S. Bonk and F. Mücklich, *Lubricants*, 2016, **4**, 2.
- 12 J. E. George, V. R. M. Rodrigues, D. Mathur, S. Chidangil and S. D. George, *Materials & Design*, 2016, **100**, 8–18.
- 13 F. Viela, I. Navarro-Baena, J. J. Hernández, M. R. Osorio and I. Rodríguez, *Bioinspiration & Biomimetics*, 2018, **13**, 026011.
- 14 I.-T. Hwang, C.-H. Jung, C.-H. Jung, J.-H. Choi, K. Shin and Y.-D. Yoo, *Journal of Biomedical Nanotechnology*, 2016, **12**, 387–393.
- 15 X.-C. Guo, W.-W. Hu, S. H. Tan and C.-W. Tsao, *Biomedical Microdevices*, , DOI:10.1007/s10544-018-0273-9.
- 16 A. Alfadhel, J. Ouyang, C. G. Mahajan, F. Forouzandeh, D. Cormier and D. A. Borkholder, *Materials & Design*, 2018, **150**, 182–187.
- 17 H. Hou, K. Hu, H. Lin, J. Forth, W. Zhang, T. P. Russell, J. Yin and X. Jiang, *Advanced Materials*, 2018, **30**, 1803463.
- 18 W. Sun and F. Q. Yang, *Express Polymer Letters*, 2018, **12**, 699–712.
- 19 D. Mampallil and H. B. Eral, *Advances in Colloid and Interface Science*, 2018, **252**, 38–54.
- 20 S. Stokols and M. H. Tuszynski, *Biomaterials*, 2006, **27**, 443–451.
- 21 A. Yamaguchi, F. Uejo, T. Yoda, T. Uchida, Y. Tanamura, T. Yamashita and N. Teramae, *Nature Materials*, 2004, **3**, 337–341.
- 22 D. Massazza, R. Parra, J. P. Busalmen and H. E. Romeo, *Energy Environ. Sci.*, 2015, **8**, 2707–2712.
- 23 D. Massazza, J. P. Busalmen, R. Parra and H. E. Romeo, *Journal of Materials Chemistry A*, 2018, **6**, 10019–10027.
- 24 S. Deville, *Advanced Engineering Materials*, 2008, **10**, 155–169.
- 25 J.-W. Kim, K. Taki, S. Nagamine and M. Ohshima, *Chemical Engineering Science*, 2008, **63**, 3858–3863.
- 26 S. Deville, *Journal of Materials Research*, 2013, **28**, 2202–2219.
- 27 H. E. Romeo, F. Trabadelo, M. Jobbágy and R. Parra, *J. Mater. Chem. C*, 2014, **2**, 2806–2814.
- 28 I. Hussain, M. Brust, A. J. Papworth and A. I. Cooper, *Langmuir*, 2003, **19**, 4831–4835.
- 29 H. Zhang, I. Hussain, M. Brust, M. F. Butler, S. P. Rannard and A. I. Cooper, *Nature Materials*, 2005, **4**, 787–793.
- 30 J.-P. Pascault, Ed., *Thermosetting polymers*, Dekker, New York, 2002.
- 31 B. Strachota, L. Matějka, A. Sikora, J. Spěváček, R. Konefał, A. Zhigunov and M. Šlouf, *Soft Matter*, 2017, **13**, 1244–1256.
- 32 H. Kirsebom, G. Rata, D. Topgaard, B. Mattiasson and I. Y. Galaev, *Macromolecules*, 2009, **42**, 5208–5214.
- 33 W. F. Schroeder, R. J. J. Williams, C. E. Hoppe and H. E. Romeo, *Journal of Materials Science*, 2017, **52**, 13669–13680.
- 34 F. I. Altuna, J. Antonacci, G. F. Arenas, V. Pettarin, C. E. Hoppe and R. J. J. Williams, *Materials Research Express*, 2016, **3**, 045003.
- 35 A. B. Leonardi, J. Puig, J. Antonacci, G. F. Arenas, I. A. Zucchi, C. E. Hoppe, L. Reven, L. Zhu, V. Toader and R. J. J. Williams, *European Polymer Journal*, 2015, **71**, 451–460.
- 36 H. H. Richardson, Z. N. Hickman, A. O. Govorov, A. C. Thomas, W. Zhang and M. E. Kordesch, *Nano Letters*, 2006, **6**, 783–788.
- 37 A. O. Govorov and H. H. Richardson, *Nano Today*, 2007, **2**, 30–38.
- 38 G. Baffou, R. Quidant and C. Girard, *Applied Physics Letters*, 2009, **94**, 153109.
- 39 E. A. Coronado, E. R. Encina and F. D. Stefani, *Nanoscale*, 2011, **3**, 4042.

- 40 A.-J. Mäki, J. Verho, J. Kreutzer, T. Rynänen, D. Rajan, M. Pekkanen-Mattila, A. Ahola, J. Hyttinen, K. Aalto-Setälä, J. Leikkala and P. Kallio, *SLAS TECHNOLOGY: Translating Life Sciences Innovation*, 2018, 247263031876871.
- 41 V. Miralles, A. Huerre, F. Malloggi and M.-C. Jullien, *Diagnostics*, 2013, **3**, 33–67.
- 42 I. E. dell'Erba, C. E. Hoppe and R. J. J. Williams, *Langmuir*, 2010, **26**, 2042–2049.
- 43 W. S. Hummers and R. E. Offeman, *Journal of the American Chemical Society*, 1958, **80**, 1339–1339.
- 44 I. Pardiñas-Blanco, C. E. Hoppe, Y. Piñeiro-Redondo, M. A. López-Quintela and J. Rivas, *Langmuir*, 2008, **24**, 983–990.
- 45 Y. Yagci, S. Jockusch and N. J. Turro, *Macromolecules*, 2010, **43**, 6245–6260.
- 46 C. R. Szczepanski and J. W. Stansbury, *European Polymer Journal*, 2015, **67**, 314–325.
- 47 G. T. Russell, D. H. Napper and R. G. Gilbert, *Macromolecules*, 1988, **21**, 2141–2148.
- 48 A. Yildirim, M. Yunusa, F. E. Ozturk, M. Kanik and M. Bayindir, *Advanced Functional Materials*, 2014, **24**, 4569–4576.
- 49 J. Drelich and E. Chibowski, *Langmuir*, 2010, **26**, 18621–18623.
- 50 F. Ghaderinezhad, R. Amin, M. Temirel, B. Yenilmez, A. Wentworth and S. Tasoglu, *Scientific Reports*, , DOI:10.1038/s41598-017-02931-6.
- 51 C. Xu, L. Cai, M. Zhong and S. Zheng, *RSC Advances*, 2015, **5**, 4770–4773.
- 52 A. W. Martinez, S. T. Phillips, G. M. Whitesides and E. Carrilho, *Analytical Chemistry*, 2010, **82**, 3–10.



Liquid flow along single aligned channels is demonstrated on micro-patterned polymeric platforms prepared by combining directional freezing and visible-light photopolymerization

